reviews

molecular pharmaceutics

Choline Phospholipid Metabolism in Cancer: Consequences for Molecular Pharmaceutical Interventions

Kristine Glunde, Ellen Ackerstaff, Noriko Mori, Michael A. Jacobs, and Zaver M. Bhujwalla*

JHU ICMIC Program, The Russell H. Morgan Department of Radiology and Radiological Science, The Johns Hopkins University School of Medicine, Baltimore, Maryland 21205

Received June 13, 2006

Abstract: Over the past decade, our program has focused on understanding the role of the physiological environment, tumor vasculature, and metabolism in several of the aggressive phenotypic traits of cancer, such as invasion and metastasis. These studies have been performed primarily with magnetic resonance (MR) imaging (MRI) and spectroscopy (MRS) on human breast and prostate cancer models. During the course of these studies, we observed specific changes in choline phospholipid metabolism associated with a more aggressive phenotype. Molecular or pharmacologic interventions that reduced this aggressiveness were also consistent with a reversal of these alterations. In this contextual review, we have outlined the insight we have gained from these studies and have discussed some of the enzymes and pathways that may present novel targets for pharmaceutical interventions in cancer.

Keywords: Choline phospholipid metabolism; cancer; magnetic resonance spectroscopy

Introduction

The choline phospholipid metabolites typically detected in high-resolution ^{1}H MR spectra are free choline (Cho), phosphocholine (PC), and glycerophosphocholine (GPC). In vivo, these three signals cannot be resolved, and a single resonance assigned to total choline-containing compounds (total choline, tCho) is detected. Similarly, in high-resolution ^{31}P MR spectra, signals from PC and phosphoethanolamine (PE), and GPC and glycerophosphoethanolamine (GPE) are detected that, at the lower spectral resolution in vivo, give rise to the phosphomonoester (PME) and phosphodiester (PDE) signals. The origins of these compounds, together with the corresponding enzymes of the choline phospholipid pathways, are shown in the schematic in Figure 1. Phosphocholine is a precursor as well as a breakdown product of the major membrane component phosphatidylcholine, whereas glycerophosphocholine is solely a membrane breakdown product. The cellular concentration of each of these choline phospholipid metabolites in Figure 1 depends on two or more enzymes, which are individually or concertedly regulated by several signal transduction pathways.[1] PE, GPE, and phosphatidylethanolamine are part of analogous ethanolamine phospholipid pathways.

Clinically, cancers developing in different organs such as primary malignant tumors in the brain,[2−4] prostate,[5−7] and breast [8−11] demonstrate an elevation in total choline. Multiple MR studies of choline phospholipid metabolism in cancer

* Corresponding author. Address: Department of Radiology, The Johns Hopkins University School of Medicine, Baltimore, MD 21205. Tel: (410)-955-9698. Fax: (410)-614-1948. E-mail: zaver@mri.jhu.edu.

(1) Glunde, K.; Jie, C.; Bhujwalla, Z. M. *Cancer Res.* **2004**, *64*, 4270−6.
(2) Barker, P. B.; Glickson, J. D.; Bryan, R. N. *Top. Magn. Reson. Imaging* **1993**, *5*, 32−45.
(3) Pouwels, P. J. W.; Frahm, J. *Magn. Reson. Med.* **1998**, *39*, 53−60.
(4) Ross, B.; Michaelis, T. *Magn. Reson. Q* **1994**, *10*, 191−247.
(5) Narayan, P.; Kurhanewicz, J. *Prostate Suppl.* **1992**, *4*, 43−50.
(6) Schick, F.; Bongers, H.; Kurz, S.; Jung, W. I.; Pfeffer, M.; Lutz, O. *Magn. Reson. Med.* **1993**, *29*, 38−43.
(7) Kurhanewicz, J.; Vigneron, D. B.; Hricak, H.; Narayan, P.; Carroll, P.; Nelson, S. J. *Radiology* **1996**, *198*, 795−805.
(8) Jagannathan, N. R.; Singh, M.; Govindaraju, V.; Raghunathan, P.; Coshic, O.; Julka, P. K.; Rath, G. K. *NMR Biomed.* **1998**, *11*, 414−422.

10.1021/mp060067e CCC: $33.50
Published on Web 09/09/2006

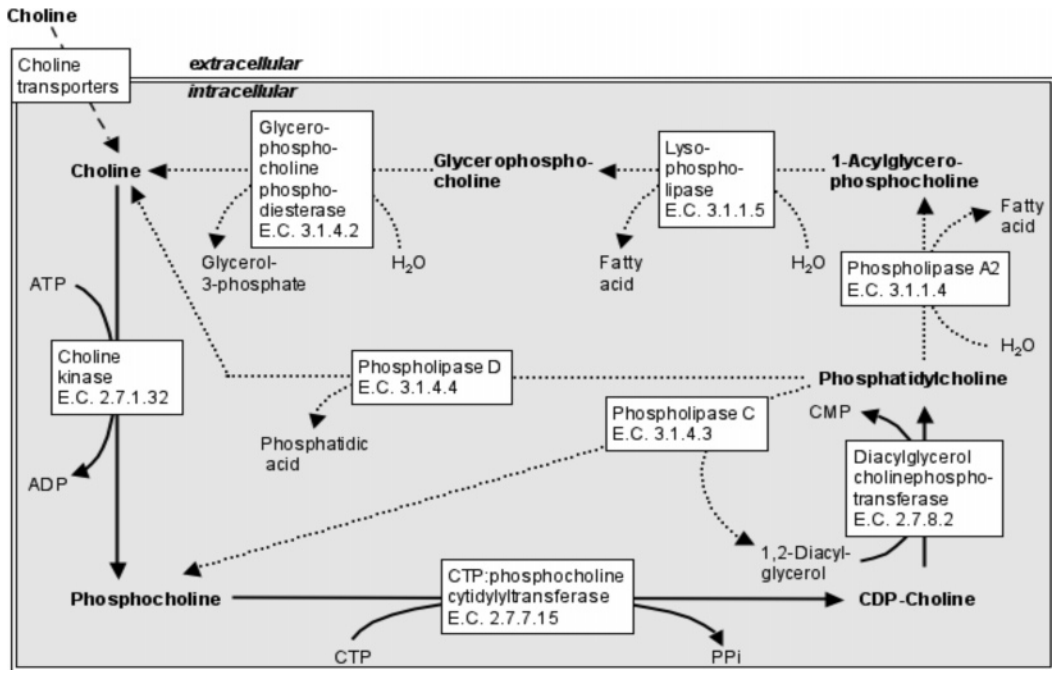

Figure 1. Biosynthetic (solid lines) and catabolic (dashed lines) enzymatic reactions in choline phospholipid metabolism. ADP, adenosine diphosphate; ATP, adenosine triphosphate; CDP, cytosine diphosphate; CMP, cytosine monophosphate; CTP, cytosine triphosphate; PPi, pyrophosphate. Adapted from ref 1.

have confirmed these findings of elevated tCho and PC in cancers.[12−18] Figure 2 gives an example of elevated total choline in clinical breast cancer.[11] This elevation of total choline is becoming an important biomarker in cancer diagnosis and can be useful in treatment planning for radiation[19] or brachytherapy.[20] Moreover, recent reports have shown the promise of MRS in assisting the evaluation of the treatment response in the brain,[21] breast,[22,23] and prostate.[24] Breast cancers responding to chemotherapy showed a significant reduction of the tCho signal, suggesting the importance of this noninvasive biomarker in monitoring response to therapy.[22] Similar reports have demonstrated that changes in both tCho and citrate detected by MRS were predictive in prostate cancer.[24,25]

Transfection of Invasive Metastatic Human Breast Cancer Cells with a Metastasis Suppressor Gene (nm23) Led to Increased GPC and Decreased PC. Our interest in choline metabolism was initiated by a ^{31}P MRS study of tumors formed in the mammary fat pad of severe combined immunesuppressed (SCID) mice by MDA-MB-435 human breast carcinoma cells transfected with cDNA encoding the wild-type nm23-H1 metastasis suppressor gene (MDA-MB-435−1β).[26] Tumors formed by MDA-MB-435 cells transfected with vector alone were used as controls (MDA-MB-435-Vβ). As shown in Figure 3, the in vivo ^{31}P MR spectra of transgene tumors formed by wild-type forms of nm23-

(9) Roebuck, J. R.; Cecil, K. M.; Schnall, M. D.; Lenkinski, R. E. *Radiology* **1998**, *209*, 269−275.
(10) Yeung, D. K.; Cheung, H. S.; Tse, G. M. *Radiology* **2001**, *220*, 40−6.
(11) Jacobs, M. A.; Barker, P. B.; Bottomley, P. A.; Bhujwalla, Z.; Bluemke, D. B. *J. Magn. Reson. Imaging* **2004**, *19*, 68−75.
(12) Negendank, W. *NMR Biomed.* **1992**, *5*, 303−24.
(13) Podo, F. *NMR Biomed.* **1999**, *12*, 413−39.
(14) Gillies, R. J.; Morse, D. L. *Annu. Rev. Biomed. Eng.* **2005**, 7, 287−326.
(15) Ronen, S. M.; Leach, M. O. *Breast Cancer Res.* **2001**, *3*, 36−40.
(16) Katz-Brull, R.; Lavin, P. T.; Lenkinski, R. E. *J. Natl. Cancer Inst.* **2002**, *94*, 1197−203.
(17) Bell, J. D.; Bhakoo, K. K. *NMR Biomed.* **1998**, *11*, 354−9.
(18) Howe, F. A.; Barton, S. J.; Cudlip, S. A.; Stubbs, M.; Saunders, D. E.; Murphy, M.; Wilkins, P.; Opstad, K. S.; Doyle, V. L.; McLean, M. A.; Bell, B. A.; Griffiths, J. R. *Magn. Reson. Med.* **2003**, *49*, 223−32.
(19) Nelson, S. J.; Graves, E.; Pirzkall, A.; Li, X.; Antiniw Chan, A.; Vigneron, D. B.; McKnight, T. R. *J. Magn. Reson. Imaging* **2002**, *16*, 464−76.
(20) Zaider, M.; Zelefsky, M. J.; Lee, E. K.; Zakian, K. L.; Amols, H. I.; Dyke, J.; Cohen, G.; Hu, Y.; Endi, A. K.; Chui, C.; Koutcher, J. A. *Int. J. Radiat. Oncol. Biol. Phys.* **2000**, *47*, 1085−96.
(21) Law, M.; Cha, S.; Knopp, E. A.; Johnson, G.; Arnett, J.; Litt, A. W. *Radiology* **2002**, *222*, 715−21.
(22) Meisamy, S.; Bolan, P. J.; Baker, E. H.; Bliss, R. L.; Gulbahce, E.; Everson, L. I.; Nelson, M. T.; Emory, T. H.; Tuttle, T. M.; Yee, D.; Garwood, M. *Radiology* **2004**, *233*, 424−31.
(23) Manton, D. J.; Chaturvedi, A.; Hubbard, A.; Lind, M. J.; Lowry, M.; Maraveyas, A.; Pickles, M. D.; Tozer, D. J.; Turnbull, L. W. *Br. J. Cancer* **2006**, *94*, 427−35.
(24) Kurhanewicz, J.; Vigneron, D. B.; Nelson, S. J. *Neoplasia* **2000**, *2*, 166−89.
(25) Mueller-Lisse, U. G.; Swanson, M. G.; Vigneron, D. B.; Hricak, H.; Bessette, A.; Males, R. G.; Wood, P. J.; Noworolski, S.; Nelson, S. J.; Barken, I.; Carroll, P. R.; Kurhanewicz, J. *Magn. Reson. Med.* **2001**, *46*, 49−57.
(26) Bhujwalla, Z. M.; Aboagye, E. O.; Gillies, R. J.; Chacko, V. P.; Mendola, C. E.; Backer, J. M. *Magn. Reson. Med.* **1999**, *41*, 897−903.

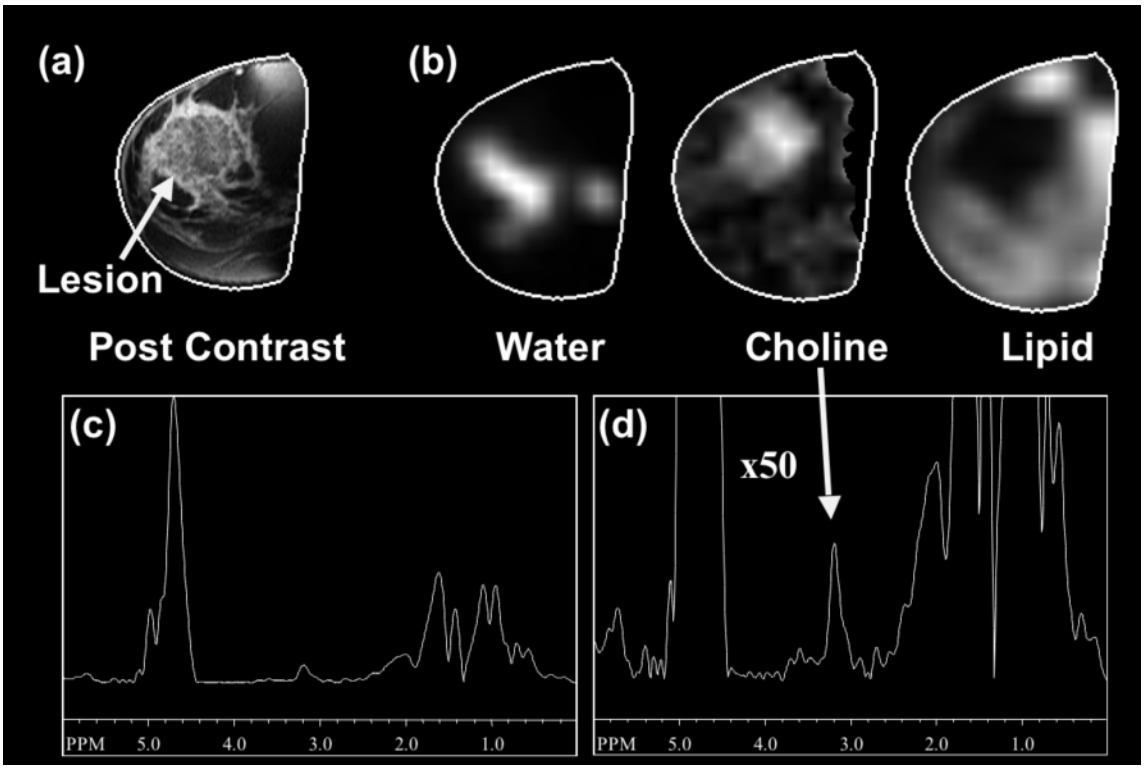

Figure 2. Proton MRI and MRSI of a 41-year-old patient with infiltrating ductal carcinoma of the breast. (a) Post contrast T_1-weighted images of the breast lesion. (b) MRSI images of water, total-choline containing compounds (choline), and lipids. (c) Representative spectrum of elevated choline (SNR = 10.6) within the lesion and (d) magnified (x50) region demonstrates a detectable choline signal. Adapted from ref 11.

H1 exhibited a significantly higher amount of PDE relative to PME levels when compared with vector control tumors. Nm23-expressing MDA-MB-435 cells had significantly lower PC levels and higher GPC levels compared to vector-transfected or wild-type MDA-MB-435 cells, as determined by high-resolution MRS of extracts.[26]

The effect of nm23 transfection on the attenuation of metastasis was confirmed by histological analysis of lung sections obtained from tumor-bearing animals (Figure 4). These changes in phospholipid metabolism detected following nm23 transfection indicate an association between choline phospholipid metabolism, invasion, and metastasis.

Human Mammary Epithelial Cells (HMECs) Exhibited an Increase of PC and Total Choline Compounds with Progression to the Malignant Phenotype. In addition, a switch from high GPC, low PC to low GPC, high PC was observed with malignant progression, supporting the observation made with the nm23-transfected cells.

We subsequently assessed PC, GPC, and tCho levels in a number of epithelial cell lines derived from reduction mammoplasty (normal) tissues and neoplastic lesions (Table 1) and investigated the effects of immortalization and oncogene transformation on phospholipid levels. Such a model has been employed to evaluate the stepwise progression in mammary epithelium from normal to malignant phenotype.[27−29] Our data suggest that phenotypic changes in phospholipids probably commence early in carcinogenesis and may, as with most other neoplastic phenotypes, be regulated by an interplay of cellular immortalization and oncogene transformation. A GPC to PC switch (Figures 5 and 6) appeared to be an early phenotypic change during carcinogenesis as observed in benzo(α)pyrene-immortalized cells, where instead of GPC, PC became the major choline phospholipid metabolite (Figures 6 and 7).[30]

Our findings suggest that normal human mammary epithelium has low steady-state levels of total choline-containing metabolites. In addition to their low total-choline containing metabolite levels (Figure 7), we also demonstrated that GPC was the major metabolite in the normal HMECs.[30] However, despite this "switch", total choline-containing metabolite levels remained low in these immortalized cells.

Transformation of 184B5 immortal cells by overexpression of the *erbB2* oncogene resulted in a dramatic increase in both the PC/GPC ratio and the total choline levels compared to the benzo(α)pyrene-immortalized cells, although total choline-containing metabolites and PC levels were still less than those of tumor-derived cells (Figures 5 and 7). *ErbB2*

(28) Stampfer, M. R.; Bartley, J. C. *Proc. Natl. Acad. Sci. U.S.A.* **1985**, 82, 2394−2398.
(29) Pierce, J. H.; Arnstein, P.; DiMarco, E.; Artrip, J.; Kraus, M. H.; Lonardo, F.; DiFiore, P. P.; Aaronson, S. A. *Oncogene* **1991**, *6*, 1189−1194.
(30) Thompson, E. W.; Torri, J.; Sabol, M.; Sommers, C. L.; Byers, S.; Valverius, E. M.; Martin, G. R.; Lippman, M. E.; Stampfer, M. R.; Dickson, R. B. *Clin. Exp. Metastasis* **1994**, *12*, 181−194.
(31) Aboagye, E. O.; Bhujwalla, Z. M. *Cancer Res.* **1999**, *59*, 80−4.

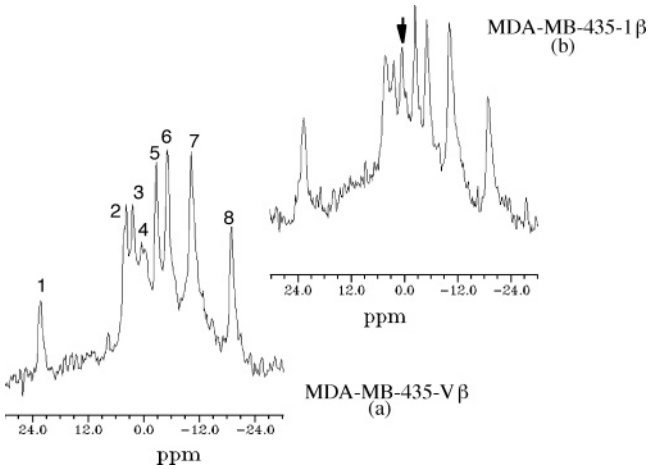

Figure 3. Representative fully relaxed ^{31}P MR spectra obtained from (a) a control vector MDA-MB-435-Vβ tumor and (b) a wild-type nm23-H1-expressing MDA-MB-435-1β tumor. Signal assignments are (1) 3-APP, (2) phosphomonoester (PME), (3) Inorganic phosphate (Pi), (4) phosphodiester (PDE), (5) phosphocreatine (PCr), (6) γ-NTP, (7) α-NTP (set to −10 ppm), and (8) β-NTP. Adapted from ref 26.

is an important (proto)oncogene that is amplified in 20%−30% of breast cancer cases and is associated with poor prognosis; amplification of this oncogene is thought to occur late in tumor progression.[31−34] Transformation of 184B5 by *erbB2* resulted in the ability of these cells to form colonies in semisolid medium and form small, low-frequency tumors with high latency in vivo.[28]

All of the breast tumor cell lines exhibited the GPC to PC switch (Figures 5−7). In addition to this switch, all breast tumor cell lines displayed significantly higher total choline-containing metabolite levels ($p < 0.05$, tumor-derived cells vs mortal cells). The increased total choline-containing metabolite levels were mainly due to an increase in PC levels and, to a lesser and variable extent, an increase in GPC levels. There was a gradual increase in both the total choline-containing metabolite levels and the PC levels as the cells acquired a malignant phenotype (normal < immortal < oncogene transformed < tumor derived) with the highly invasive metastatic cell lines showing the highest levels. The high total choline content in the tumorigenic cells may be related to the multiple genetic changes that are associated with the multistep process of carcinogenesis[32] and may be related to the progressive ability of these cells to gain anchorage-independent growth, form primary tumors in immune-compromised mice, and finally metastasize.

Treatment of Malignant HMECs with an Antiinflammatory Agent, Indomethacin, Reverted the High PC, Low GPC Pattern to a Low PC, High GPC Pattern Indicative of a Less Malignant Phenotype. Several studies have shown that the nonsteroidal antiinflammatory agent indomethacin can inhibit the invasive and metastatic behavior of human breast cancer cells.[35] We therefore treated malignant as well as nonmalignant HMECs with indomethacin to determine its effect on choline phospholipid metabolism. We performed real-time monitoring of choline compounds of intact cells during treatment with indomethacin using our MR-compatible cell perfusion system. Proton MR spectra from extracts of cells growing in tissue culture flasks were also obtained. For the extract studies, cells were treated with 50 μM indomethacin for 18 h or 300 μM of indomethacin for a period of 3 h. Parallel control experiments of untreated cells were performed over the same time period for both isolated perfused cell studies as well as the extract studies.[36,37] Treatment with indomethacin resulted in a significant reduction of PC and an increase of GPC; control spectra obtained over a similar time period showed no changes. In intact cells, the drop in PC and increase in GPC were evident within 80 min following addition of indomethacin to the medium.[36] Proton spectra obtained from cell extracts of MDA-MB-435 cells (Figure 8) also showed a significant increase of GPC and decrease of PC following treatment with indomethacin.

Treatment with indomethacin also resulted in increased expression of nm23.[37] A significant correlation was observed between cyclooxygenase (COX)-1, but not COX-2 levels, and total choline in HMECs.[37] These data suggest that choline phospholipid metabolites may be related, in part, to the inflammatory state of human breast cancer cells. We are currently using ^{13}C MRS of HMECs labeled with [1,2-^{13}C]-choline in combination with microarray analyses to further understand alterations in choline phospholipids following treatment with indomethacin.

We have also characterized changes in invasion of a malignant and invasive breast cancer cell line, MDA-MB-435, following exposure to indomethacin using our MR-compatible cell invasion assay.[38] Shown in Figure 9 are images of MDA-MB-435 cells with (lower panel) or without indomethacin treatment (upper panel). The images in Figure 9 display a chamber containing reconstituted basement membrane (Matrigel) that invasive cancer cells typically degrade within a 72 h period as apparent in the upper panel. With slow-release indomethacin pellets delivering indomethacin into the medium, this degradation of Matrigel by breast cancer cells was reduced significantly as evident from the images in the lower panel in Figure 9.[38]

(31) Dickson, R. B.; Salamon, D. S.; Lippman, M. E. *Cancer Treat. Res.* **1992**, *61*, 249−273.
(32) Beckman, M. W.; Niederacher, D.; Schnurch, H. G.; Guesterson, B. A.; Bender, H. G. *J. Mol. Med.* **1993**, *1997*, 429−437.
(33) Adnane, J.; Gaudray, P.; Simon_lafontaine, J.; Jeanteur, P.; Theillet, C. *Oncogene* **1989**, *4*, 1389−1395.
(34) Slamon, D. J.; Clark, G. M.; Wong, S. G.; Levin, W. J.; Ulrich, A.; McGuire, W. L. *Science* **1987**, *235*, 177−182.
(35) Reich, R.; Martin, G. R. *Prostaglandins* **1996**, *51*, 1−17.
(36) Glunde, K.; Ackerstaff, E.; Natarajan, K.; Artemov, D.; Bhujwalla, Z. M. *Magn. Reson. Med.* **2002**, *48*, 819−825.
(37) Natarajan, K.; Mori, N.; Artemov, D.; Bhujwalla, Z. M. *Neoplasia* **2002**, *4*, 409−16.
(38) Ackerstaff, E.; Artemov, D.; Bhujwalla, Z. M. In *Indomethacin reduces the invasion of the human breast cancer cell line MDA-MB-435*, poster no. 2157. Tenth scientific meeting of the *Intl. Soc. Magn. Reson. Med.*, Honolulu, Hawaii, 2002.

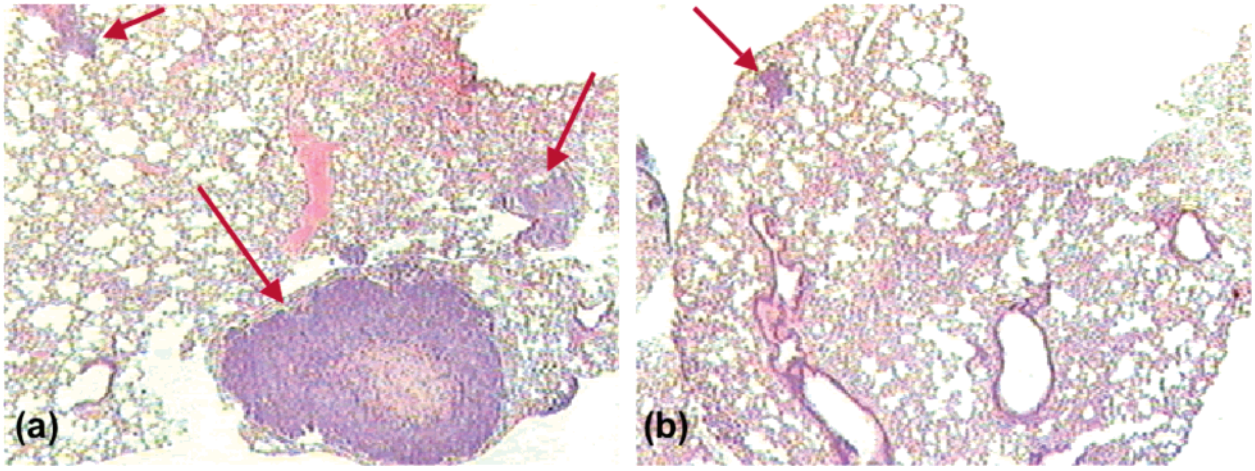

Figure 4. Photomicrographs demonstrating the marked differences in metastatic nodules in lung sections obtained from mice bearing control vector MDA-MB-435-Vβ and wild-type nm23-H1-expressing MDA-MB-435-1β tumors. Low power photomicrographs of representative 5-μm-thick hematoxylin and eosin stained lung sections obtained from a mouse with (a) an MDA-MB-435-Vβ tumor and a mouse with (b) an MDA-MB-435−1β tumor. Metastatic nodules are marked by arrows. Adapted from ref 26.

Table 1. Characteristics of HMECs in Figures 5−7[a]

cell type	phenotype
normal human mammary epithelial cells (HMEC)	
184	senescent, ADG¶
48	senescent, ADG
spontaneously immortalized HMEC	
MCF-12A	immortal, ADG
benzo[*a*]pyrene immortalized HMEC	
184A1	immortal, ADG
184B5	immortal, ADG
oncogene-transformed HMEC	
184B5-*erbB2*	immortal, AIG†, forms low frequency, high latency tumors
breast cancer cells	
SKBR3	AIG, tumorigenic, lowly metastatic
MCF7	AIG, tumorigenic, lowly metastatic
MDA-MB-231	AIG, tumorigenic, highly metastatic
MDA-MB-435	AIG, tumorigenic, highly metastatic

[a] Adapted from ref 30. ¶ADG, anchorage-dependent growth; † AIG, anchorage-independent growth.

Human Prostatic Epithelial Cells (HPCs) also Exhibit an Increase of Total Choline Compounds with Progression to the Malignant Phenotype. We also examined a panel of normal human prostate cells and prostate cancer cells (Table 2) derived from metastases by ^{1}H MRS to determine if malignant transformation of human prostate cells results in an alteration of choline compounds. Human prostate cells (HPCs) derived from metastases exhibit significantly higher PC and total choline levels compared to normal prostate epithelial and stromal cells (Figures 10 and 11).[39]

However, HPCs did not exhibit the switch from high GPC, low PC to low GPC, high PC detected in HMECs with malignant progression. These data suggest that a high PC, rather than GPC, level is primarily related to malignancy.[39]

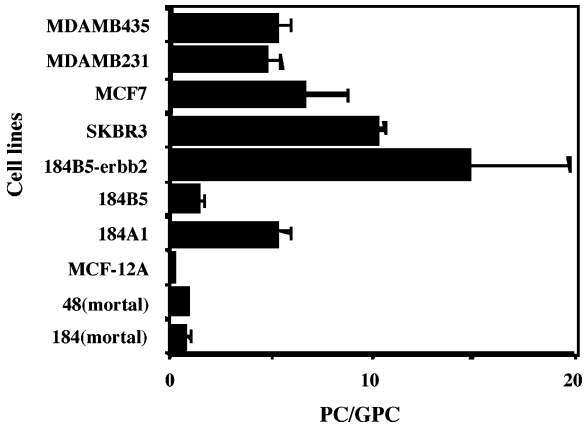

Figure 5. PC/GPC ratios in a panel of cell lines representing various stages of breast carcinogenesis. Error bars represent ±SD. There was a statistically significant difference in the PC/GPC ratio ($p < 0.05$) between finite lifespan vs tumor-derived cells, 184 strain vs 184A1 cell line, and 184B5 vs 184B5-*erbB2* cell lines. Adapted from ref 30.

Loss of p53 Function in Colon Cancer Cells Results in Increased PC and Total Choline. Human cancers that contain a p53 mutation are more aggressive, and more often fatal. Human colon carcinoma cell lines HCT116 containing a wild-type p53 (p53+/+) or a disrupted p53 (p53−/−) gene were gifts from Dr. B. Vogelstein.[40] We characterized the choline phospholipid compounds of these HCT116 human colon cancer cells with (p53+/+) and without p53 (p53−/−) and observed that the loss of the p53 function resulted in choline phospholipid changes such as increased PC and total choline (Figures 12 and 13), which were consistent with increased malignancy.[41]

(39) Ackerstaff, E.; Pflug, B. R.; Nelson, J. B.; Bhujwalla, Z. M. *Cancer Res.* **2001**, *61*, 3599−603.
(40) Bunz, F.; Dutriaux, A.; Lengauer, C.; Waldman, T.; Zhou, S.; Brown, J. P.; Sedivy, J. M.; Kinzler, K. W.; Vogelstein, B. *Science* **1998**, *282*, 1497−501.

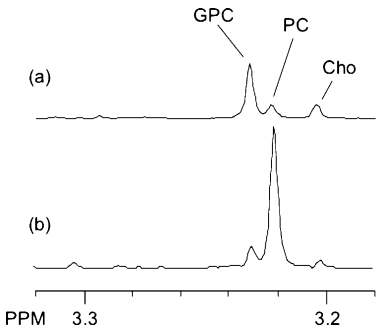

Figure 6. Typical ^{1}H MR spectra obtained from perchloric acid extracts of (a) MCF-12A human mammary epithelial cells and (b) MDA-MB-231 breast cancer cells in culture. Adapted from ref 30.

Treatment of Human Vascular Endothelial Cells (HUVECs) with Conditioned Medium Derived from Human Breast Cancer Cells Led to Increased PC Levels as well as an Increased PC/GPC Ratio in the HUVECs. Because endothelial cells form a key component of tumor vasculature, we used MRS to characterize the choline phospholipid metabolite profile of human umbilical vein endothelial cells (HUVECs).[42] We determined the effect of conditioned media obtained from a malignant cell line on choline phospholipid metabolites in HUVECs. Treatment with medium preconditioned by MDA-MB-231 cancer cells increased PC and decreased GPC levels in HUVECs (Figure 14[42]). These results demonstrate that cancer cells secreted growth factors and/or other molecules that influenced the choline phospholipid metabolites of HUVECs and that the altered choline phospholipid metabolism of tumors may occur through either paracrine or autocrine signaling. These data also suggest that cancer cell−endothelial cell interaction may be associated with choline phospholipid metabolism.[42]

Overall, the data presented indicate that diverse molecular alterations such as nm23 expression, p53 expression, and malignant transformation arrive at a common endpoint in choline phospholipid metabolism and demonstrate the important role of choline phospholipids and their metabolites in cancer.

In addition to our data presented here, several other studies have also shown elevation of PC levels with malignant transformation. High PC levels were observed in ^{31}P MR spectra of three breast cancer cell lines (21PT, 21NT, and 21MT-2) established from the same patient when compared to a normal breast epithelial cell strain (76N).[43] These changes were reflected as a significant decrease in the GPC/PC ratios of primary (21PT, 21NT) and metastatic tumor (21MT-2) cell lines in comparison to the normal cell strain. 21MT-2, the metastatic cell line, also showed a significant decrease in the GPC/PC ratio compared to the primary breast cell lines, 21PT and 21NT. Similarly, a high PC/GPC ratio was observed for a series of human tumor lines of neuronal origin when compared to primary cultures of the central and peripheral nervous system or to normal tissue obtained from brain biopsy extracts.[44] Thus, malignant transformation is accompanied by an elevation of PC. Conversely, growth arrest has been shown to reduce the PC/GPC ratio. Treatment of MCF-7 cells with tumor necrosis factor-alpha, which induces cell cycle arrest and apoptosis, resulted in a decrease of PC.[45] Collectively, these data provide a strong rationale to target enzymes in choline phospholipid metabolism.

Potential Targets for Molecular Pharmaceutical Intervention. Altering the expression or activity of enzymes involved in choline phospholipid metabolism may provide novel therapeutic strategies for anticancer treatment. An overview of differentially expressed genes involved in causing the aberrant choline phospholipid metabolism in human MDA-MB-231 breast cancer cells compared to human MCF-12A mammary epithelial cells is given in Table 3.[1] The altered choline phospholipid metabolism observed in cancer cells is, at least in part, caused by increased expression and activity of choline kinase,[46] a higher rate of choline transport,[47] and phosphatidylcholine (PtdCho)-specific phospholipase A_2, D, and C activity.[48−50] A few targets in choline phospholipid metabolism have been explored for anticancer treatment. PtdCho-specific phospholipase D (PC-PLD) plays an important role in cell proliferation and oncogenic signaling and was suggested as a potential target for therapeutic intervention in breast cancers.[51−53] Inhibition of PC−PLD activity correlated with decreased tumor invasion.[54] Choline kinase, the enzyme of the first step in the Kennedy pathway, is responsible for generating PC from free choline (see Figure 1), and has been explored as a potential target for anticancer therapy as discussed in the following section. Enzymes in choline phospholipid metabolism can either be targeted by

(41) Mori, N.; Delsite, R.; Natarajan, K.; Kulawiec, M.; Bhujwalla, Z. M.; Singh, K. K. *Mol. Imaging* **2004**, *3*, 319−23.
(42) Mori, N.; Natarajan, K.; Chacko, V. P.; Artemov, D.; Bhujwalla, Z. M. *Mol. Imaging* **2003**, *2*, 124−30.
(43) Singer, S.; Souza, K.; Thilly, W. G. *Cancer Res.* **1995**, *55*, 5140−5.
(44) Bhakoo, K. K.; Williams, S. R.; Florian, C. L.; Land, H.; Noble, M. D. *Cancer Res.* **1996**, *56*, 4630−5.
(45) Bogin, L.; Papa, M. Z.; Polak-Charcon, S.; Degani, H. *Biochim. Biophys. Acta* **1998**, *1392*, 217−32.
(46) Ramirez de Molina, A.; Gutierrez, R.; Ramos, M. A.; Silva, J. M.; Silva, J.; Bonilla, F.; Sanchez, J. J.; Lacal, J. C. *Oncogene* **2002**, *21*, 4317−22.
(47) Katz-Brull, R.; Degani, H. *Anticancer Res.* **1996**, *16*, 1375−80.
(48) Noh, D. Y.; Ahn, S. J.; Lee, R. A.; Park, I. A.; Kim, J. H.; Suh, P. G.; Ryu, S. H.; Lee, K. H.; Han, J. S. *Cancer Lett.* **2000**, *161*, 207−14.
(49) Guthridge, C. J.; Stampfer, M. R.; Clark, M. A.; Steiner, M. R. *Cancer Lett.* **1994**, *86*, 11−21.
(50) Iorio, E.; Mezzanzanica, D.; Alberti, P.; Spadaro, F.; Ramoni, C.; D'Ascenzo, S.; Millimaggi, D.; Pavan, A.; Dolo, V.; Canevari, S.; Podo, F. *Cancer Res.* **2005**, *65*, 9369−76.
(51) Foster, D. A.; Xu, L. *Mol Cancer Res.* **2003**, *1*, 789−800.
(52) Rodriguez-Gonzalez, A.; Ramirez de Molina, A.; Benitez-Rajal, J.; Lacal, J. C. *Prog. Cell Cycle Res.* **2003**, *5*, 191−201.
(53) Steed, P. M.; Chow, A. H. *Curr. Pharm. Biotechnol.* **2001**, *2*, 241−56.
(54) Pai, J. K.; Frank, E. A.; Blood, C.; Chu, M. *Anticancer Drug Des.* **1994**, *9*, 363−72.

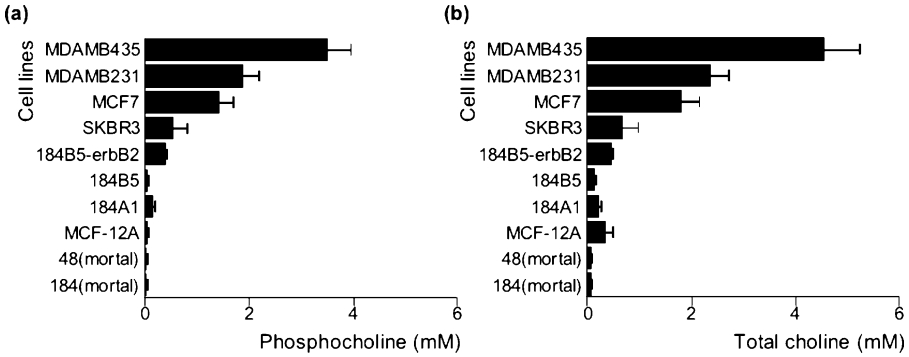

Figure 7. (a) Phosphocholine (PCho) and (b) total choline-containing metabolite (phosphocholine + glycerophosphocholine + choline) levels in a panel of cell lines representing various stages of breast carcinogenesis. Error bars represent ±SD. Adapted from ref 30.

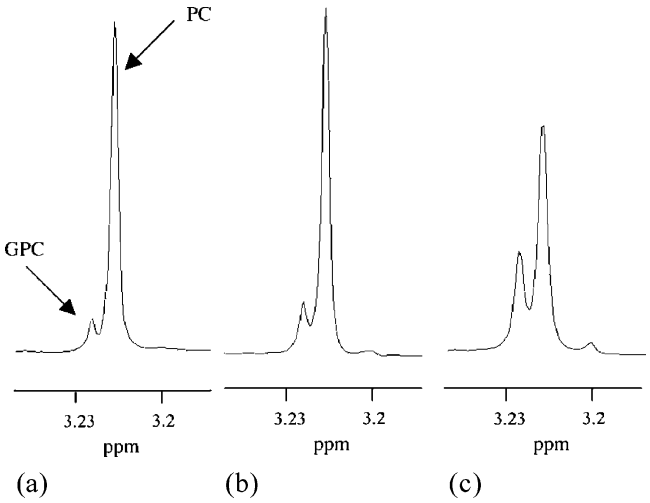

Figure 8. Proton NMR spectra of MDA-MB-435 cell extracts. Proton spectra are from (a) untreated cells, (b) cells treated with 50 μM indomethacin for 18 h, and (c) cells treated with 300 μM indomethacin for 3 h. Adapted from ref 37.

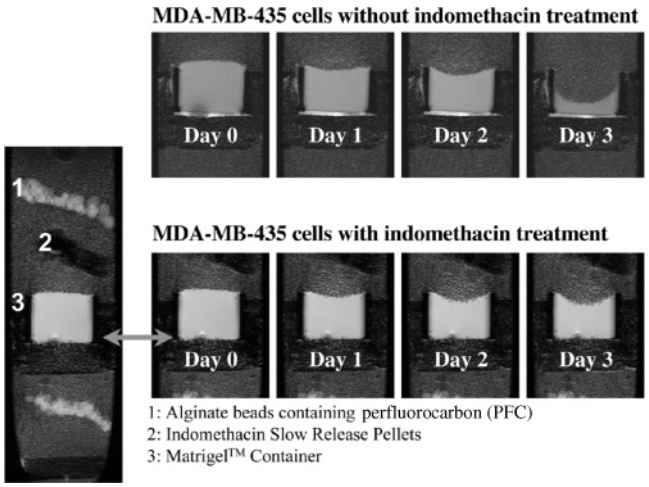

Figure 9. T_1-weighted ^{1}H MR images comparing the degradation of the ECM gel by MDA-MB-435 cells under control conditions (top panel) and during indomethacin treatment (bottom panel). The MR image on the left shows the content of the sample during the indomethacin treatment (0.5 μM). Adapted from ref 38.

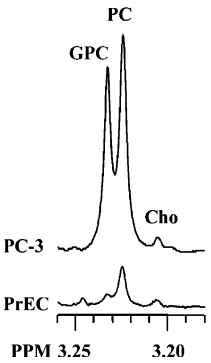

Figure 10. Qualitative differences in expanded 1D ^{1}H MR spectra of the choline-containing region obtained from perchloric acid extracts of PrEC and PC-3 cells. Malignant PC-3 cells show elevated PC and GPC compared to prostate epithelial cells (PrEC). Adapted from ref 39.

Table 2. Phenotype and Origin of the Panel of HPCs[a]

cell line	phenotype	origin
PrSC	senescent	prostate stromal cells (fibroblastic)
PrEC	senescent	prostate epithelial cells
LNCaP	malignant	lymph node metastasis
LAPC-4	malignant	lymph node metastasis
DU-145	malignant	brain metastasis
TSU	malignant	lymph node metastasis
PC-3	malignant	bone metastasis
PPC-1	malignant	stage D2 prostatic carcinoma

[a] Adapted from ref 39.

chemical enzyme inhibitors or more specifically by small interfering RNA or cDNA, which can target a single or multiple targets using viral or liposomal delivery mechanisms.

Targeting Choline Kinase in Cancer Cells. We initially focused on choline kinase because previous studies demonstrated that various growth factors,[55] chemical carcinogens,[56] and oncogenes[57,58] enhanced the activity/expression of choline kinase in mammalian cells. Further convincing data of

(55) Warden, C. H.; Friedkin, M. *J. Biol. Chem.* **1985**, *260*, 6006−11.
(56) Tadokoro, K.; Ishidate, K.; Nakazawa, Y. *Biochim. Biophys. Acta* **1985**, *835*, 501−13.
(57) Ratnam, S.; Kent, C. *Arch. Biochem. Biophys.* **1995**, *323*, 313−22.

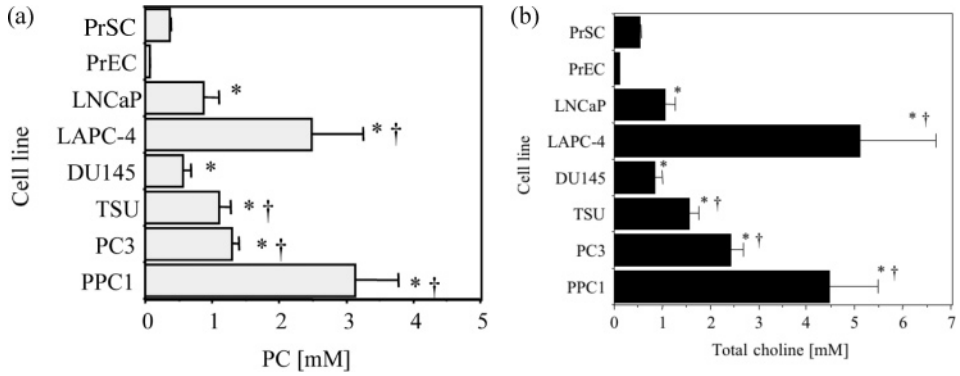

Figure 11. (a) PC concentrations and (b) total choline concentrations for a panel of HPCs comparing normal prostate cells of stromal and epithelial origin with androgen-dependent and -independent prostate tumor cells, obtained from ^{1}H MR spectra of perchloric acid extracts. Significant differences between tumor cell lines and the normal PrEC cells are marked by * ($p < 0.05$), and between the PrSC cells are marked by † ($p < 0.05$). Values are mean ±SD; three independent extracts per line. Adapted from ref 39.

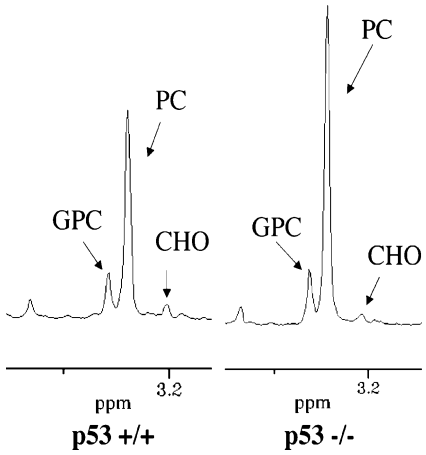

Figure 12. Representative ^{1}H MR spectra of the phospholipid region of HCT116 p53+/+ and HCT116 p53−/− cell extracts, obtained from identical cell numbers. Adapted from ref 41.

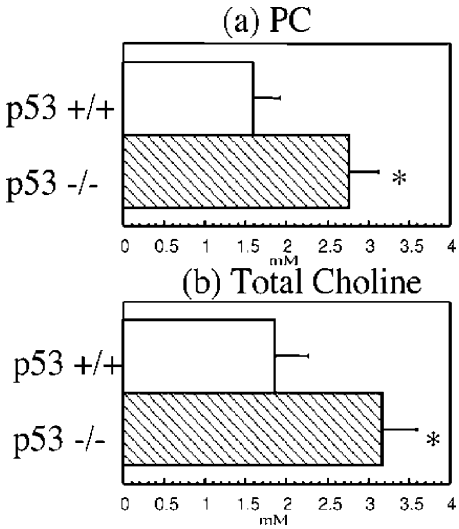

Figure 13. (a) Phosphocholine levels in HCT116 p53+/+ and HCT116 p53−/− cell extracts ($n = 7$); (b) Total choline (CHO + PC +GPC) levels in p53+/+ and p53−/− cell extracts ($n = 7$). *: significantly different compared to p53+/+ ($p < 0.05$). Bars represent mean ± SD. Adapted from ref 41.

the role of choline kinase in breast cancer was published recently in a study, which demonstrated an increase in choline kinase activity in tumoral tissue when compared to normal tissue.[46] A significant association between choline kinase enzymatic activity with histological tumor grade and with estrogen receptor (ER)-negative tumors was also observed in these studies. Overexpression of choline kinase has also been observed in several human cancer cells lines, including the ones used by us, as well as in lung, prostate, and colorectal human cancers.[59] These observations are consistent with the elevated PC levels observed by us in a panel of human breast and prostate cancer cell lines, using ^{1}H MRS. Chemical compounds such as hemicholinium-3 (HC-3) used to inhibit choline kinase activity demonstrated anti-mitogenic activity.[60] HC-3, however, also exhibits significant neurotoxicity due to inhibition of choline uptake and depletion of acetylcholine in neurons.[61,62] Improved choline kinase inhibitors, which do not interfere with other mitogenic signaling pathways, also exhibited a similar anti-mitogenic and anti-proliferative effect.[60,63] These new choline kinase inhibitors are significantly less toxic and can be administered in mice.[64] Administration of such compounds, for example MN58b, with daily doses of 3 mg/kg for 4 days with a gap of 3 days between each treatment resulted in an inhibition of tumor growth by 70%.[64,65] MN58b administration in cultured tumor cells and in vivo resulted in decreased PC, total choline, and PME levels, which may be used as

(58) Ramirez de Molina, A.; Penalva, V.; Lucas, L.; Lacal, J. C. *Oncogene* **2002**, *21*, 937−46.
(59) Ramirez de Molina, A.; Rodriguez-Gonzalez, A.; Gutierrez, R.; Martinez-Pineiro, L.; Sanchez, J.; Bonilla, F.; Rosell, R.; Lacal, J. *Biochem. Biophys. Res. Commun.* **2002**, *296*, 580−3.
(60) Hernandez-Alcoceba, R.; Saniger, L.; Campos, J.; Nunez, M. C.; Khaless, F.; Gallo, M. A.; Espinosa, A.; Lacal, J. C. *Oncogene* **1997**, *15*, 2289−301.
(61) Craig, C. R.; Curtis, D. R.; Lodge, D. *J. Physiol.* **1977**, *264*, 367−77.
(62) Cannon, J. G. *Med. Res. Rev.* **1994**, *14*, 505−31.

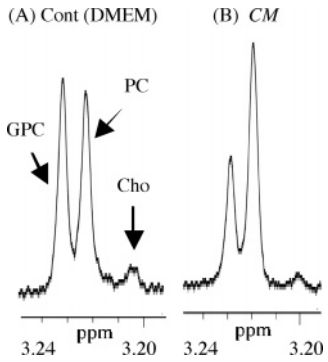

Figure 14. Representative ^{1}H MR spectra from the choline phospholipid region of PCA extracts of HUVECs cultured for 18 h with (A) control (DMEM) and (B) *CM* (conditioned medium obtained following incubation over 48 h of MDA-MB-231 cells). Spectra were acquired with 30° flip angle, 6000 Hz sweep width, 4.7 s repetition time, 32 K block size, and 128−512 scans. Spectra are expanded to display signals from PC, GPC, and Cho region only. Adapted from ref 42.

noninvasive pharmacodynamic biomarkers of tumor response following treatment with choline kinase inhibitors.[65] However, even with the newer compounds, toxicity still limits the dose that can be administered. With the explosion of powerful molecular biology techniques, it is now possible to target choline kinase using a molecular biology-based approach. Cells can be made to express small interfering RNA (siRNA), which would inhibit the expression of a specific enzyme such as choline kinase.

We therefore generated stable clones of MDA-MB-231 breast cancer cells expressing siRNA targeting choline kinase (designated U6-shRNA-Chk). MDA-MB-231 breast cancer cells expressing this U6-shRNA-Chk vector contained significantly decreased choline kinase mRNA and protein levels reflected by significantly decreased total choline and PC levels (Figure 15).[66]

Table 3. Gene Expression Differences in MDA-MB-231 Breast Cancer Cells versus MCF-12A Human Mammary Epithelial Cells[a]

gene	MCF-12A	MDA-MB-231	fold change (90% CI)
choline kinase (2 independent probe sets)	39 ± 13	166 ± 29	4.27 (2.44 to 9.91)
lysophospholipase 1 (2 independent probe sets)	684 ± 29	174 ± 11	−3.94 (−3.47 to −4.50)
phospholipase A2, group IVA (cytosolic, calcium-dependent)	98 ± 15	20 ± 3	−4.98 (−3.41 to −7.45)
pancreas-enriched phospholipase C	19 ± 9	43 ± 8	2.28 (1.14 to 9.98)
phospholipase C, beta 3, neighbor pseudogene	209 ± 45	577 ± 87	2.76 (1.82 to 4.51)
phospholipase D1 (phosphatidylcholine-specific)	35 ± 4	12 ± 4	−2.85 (−1.78 to −5.89)

[a] Significantly over- or underexpressed genes (more than a 2-fold difference) involved in choline phospholipid metabolism are listed. Only well-characterized human genes are displayed. CI represents confidence interval. Expression index values presented as relative units are mean ± SD. Adapted from ref 1

We observed that proliferation was significantly ($p < 0.001$, $n = 5$) slower in MDA-MB-231 breast cancer cells stably expressing U6-shRNA-Chk compared to empty-vector controls (Figure 16a). The cell-doubling time of U6-shRNA-Chk expressing MDA-MB-231 cells was significantly longer

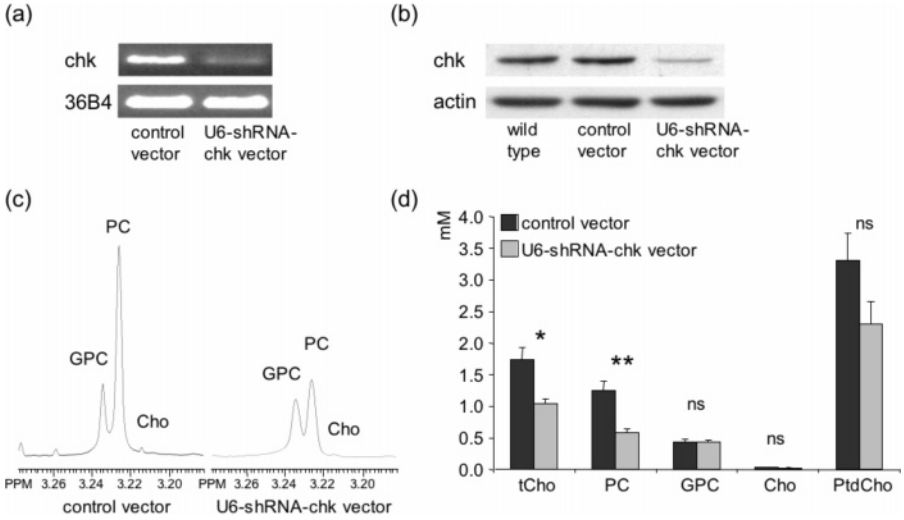

Figure 15. MDA-MB-231 breast cancer cells expressing siRNA-Chk vector. (a) RT-PCR of clones containing either empty vector or siRNA-Chk vector. The choline kinase (Chk) message is decreased significantly in siRNA-Chk vector expressing MDA-MB-231 cells compared to empty-vector control. (b) Western blot using Chk antibody demonstrates low Chk protein levels in siRNA-Chk expressing cells, while empty-vector control contains Chk levels comparable to wild-type MDA-MB-231 breast cancer cells. (c) Corresponding expanded regions of ^{1}H MR spectra show that siRNA-Chk expressing cells (right) contain significantly decreased PC levels compared to empty-vector control cells (left). (d) Corresponding quantitation of ^{1}H MR specra from water-soluble and lipid phase ($n = 3$). Values represent mean ± SD. Adapted from ref 66.

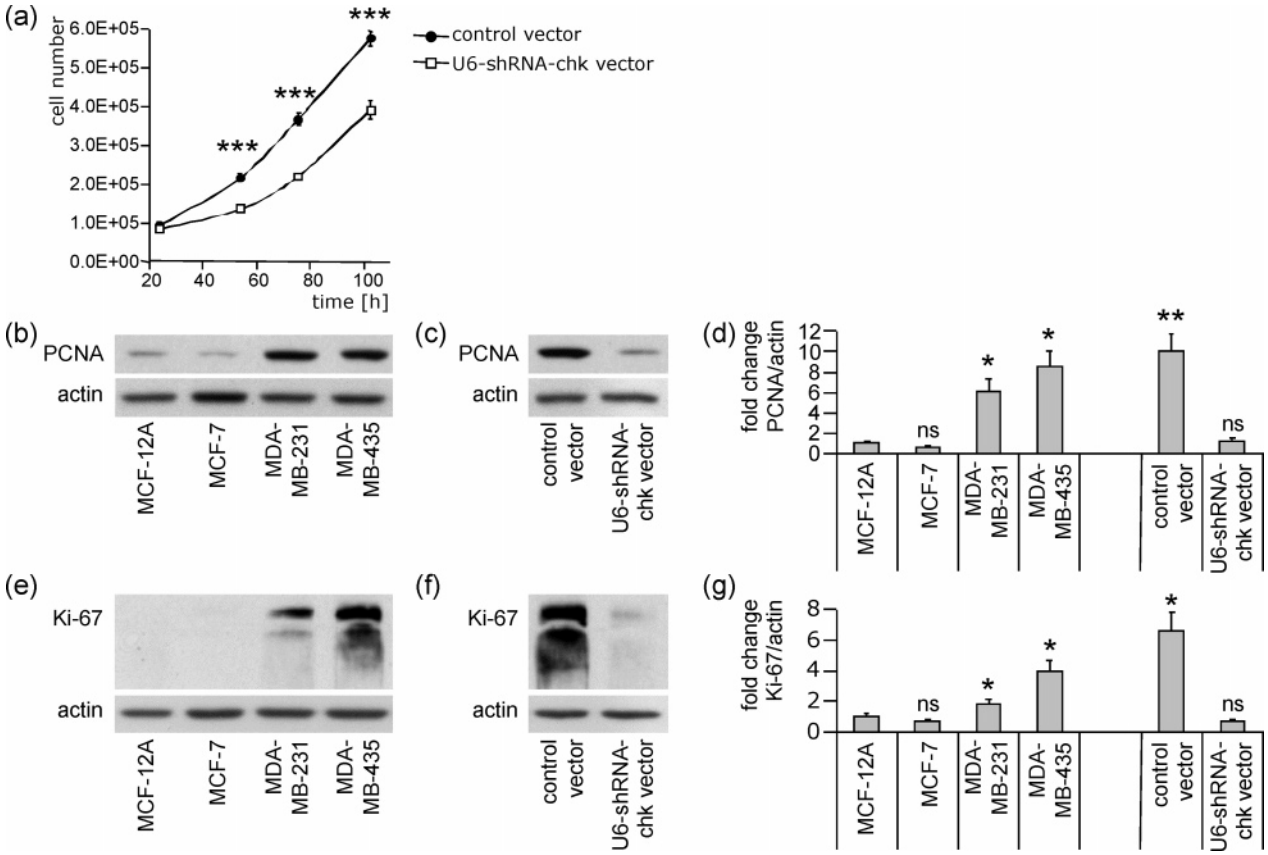

Figure 16. Decreased proliferation in MDA-MB-231 breast cancer cells stably expressing U6-shRNA-Chk. (a) The proliferation rate of MDA-MB-231 cells containing stably knocked-down Chk was decreased significantly compared to vector control. Values represent mean ± SD. (b) For comparison, PCNA immunoblotting was performed in a panel of human breast epithelial cell lines exhibiting different degrees of malignancy. Nonmalignant HMECs MCF-12A and poorly metastatic MCF-7 breast cancer cells exhibited low levels of PCNA compared to the high PCNA expression levels detected in the invasive and metastatic breast cancer cell lines, MDA-MB-231 and MDA-MB-435. (c) Stable knockdown of Chk in MDA-MB-231 cells resulted in significantly decreased PCNA levels compared to control vector cells. (d) Densitometry of Western blots demonstrates semiquantitative fold changes relative to MCF-12A cells ($n = 3$). Relative fold changes in PCNA were normalized to the PCNA immunoreactive band in MCF-12A cells, which was set to 1. Values represent mean ± SD. (e) Ki-67 expression was low in nonmalignant (MCF-12A) and poorly invasive breast epithelial cells (MCF-7), compared to the invasive breast cancer cells (MDA-MB-231 and MDA-MB-435). (f) Stable Chk knockdown in MDA-MB-231 cells resulted in significantly decreased Ki-67 expression levels compared to control vector. Actin was probed as a loading control in all blots. (g) Densitometry of Western blots demonstrated semiquantitative changes relative to MCF-12A cells ($n = 3$). Relative fold changes in Ki-67 were normalized to the Ki-67 immunoreactive band in MCF-12A cells, which was set to 1. Values represent mean ± SD. * indicates $p < 0.05$, ** indicates $p < 0.01$, *** indicates $p < 0.001$, and ns indicates not significant compared to MCF-12A. Adapted from ref 66.

(34.7 h) than that for MDA-MB-231 cells with the control vector (28.8 h). Expression levels of two proliferation markers, proliferating cell nuclear antigen (PCNA)[67,68] (Figure 16b) and Ki-67[69] (Figure 16e), were significantly ($p < 0.01$ and $p < 0.05$, respectively, $n = 3$; Figure 16d and g) higher in the two metastatic human breast cancer cell lines MDA-MB-231 and MDA-MB-435 compared to the poorly metastatic human breast cancer cell line MCF-7 and the nonmalignant HMEC line MCF-12A (Figure 16). Both PCNA (Figure 16c) and Ki-67 (Figure 16f) were significantly ($p < 0.01$, $n = 3$; Figure 16d, g) underexpressed in MDA-MB-231 breast cancer cells stably expressing U6-shRNA-Chk compared to empty-vector MDA-MB-231 cells. PCNA and Ki-67 protein expression levels in MDA-MB-231 cells expressing U6-shRNA-Chk were comparable to the expression levels in MCF-12A HMECs (Figure 16b−g).

(63) Campos, J. M.; Nunez, M. C.; Sanchez, R. M.; Gomez-Vidal, J. A.; Rodriguez-Gonzalez, A.; Banez, M.; Gallo, M. A.; Lacal, J. C.; Espinosa, A. *Bioorg. Med. Chem.* **2002**, *10*, 2215−31.
(64) Hernandez-Alcoceba, R.; Fernandez, F.; Lacal, J. C. *Cancer Res.* **1999**, *59*, 3112−8.
(65) Al-Saffar, N. M.; Troy, H.; Ramirez de Molina, A.; Jackson, L. E.; Madhu, B.; Griffiths, J. R.; Leach, M. O.; Workman, P.; Lacal, J. C.; Judson, I. R.; Chung, Y. L. *Cancer Res.* **2006**, *66*, 427−34.
(66) Glunde, K.; Raman, V.; Mori, N.; Bhujwalla, Z. M. *Cancer Res.* **2005**, *65*, 11034−43.
(67) Heimann, R.; Hellman, S. *Eur. J. Cancer* **2000**, *36*, 1631−9.
(68) Maga, G.; Hubscher, U. *J. Cell Sci.* **2003**, *116*, 3051−60.
(69) Scholzen, T.; Gerdes, J. *J. Cell Physiol.* **2000**, *182*, 311−22.

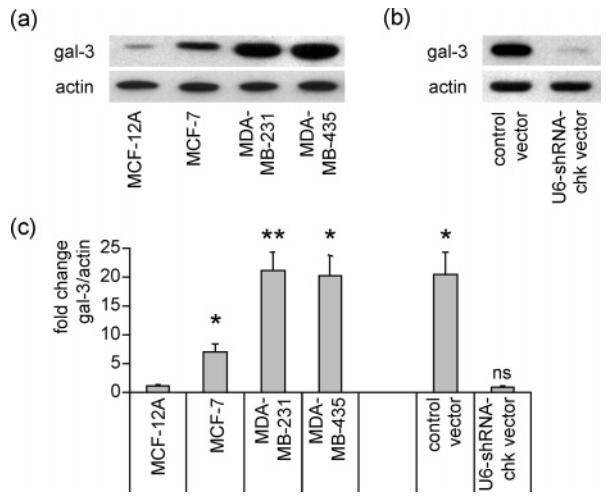

Figure 17. Decreased galectin-3 expression in MDA-MB-231 breast cancer cells containing stably knocked-down Chk. (a) Low galectin-3 expression levels were detected in nonmalignant MCF-12A HMECs and poorly metastatic MCF-7 breast cancer cells, whereas high galectin-3 expression levels were detected in the invasive/metastatic breast cancer cell lines MDA-MB-231 and MDA-MB-435. (b) Stable Chk knockdown in MDA-MB-231 cells resulted in a significant reduction of galectin-3 expression. Actin was probed as a loading control in all blots. (c) Densitometry of Western blots demonstrated semiquantitative changes relative to MCF-12A cells ($n = 3$). Relative fold changes in Galectin-3 were normalized to the Gal-3 immunoreactive band in MCF-12A cells, which was set to 1. Values represent mean ± SD, * indicates $p < 0.05$, and ns indicates not significant compared to MCF-12A. Adapted from ref 66.

To test for differentiation of the different breast epithelial cell lines and the choline kinase knockdown clones, we probed for galectin-3 protein expression by SDS-PAGE followed by immunoblotting. Galectin-3 is involved in several biological processes, including cell adhesion, migration, cell growth, differentiation, apoptosis, tumor progression, and metastasis in human breast epithelial cells.[70−73] Figure 17a demonstrates that nonmalignant immortalized MCF-12A HMECs expressed almost undetectable levels of galectin-3, compared to MCF-7, MDA-MB-231, and MDA-MB-435 breast cancer cells, where progressively increasing galectin-3 levels matched the decreasing differentiation of these cell lines. Galectin-3 protein expression levels were significantly ($p < 0.05$, $n = 3$) higher in all three breast cancer cell lines compared to MCF-12A (Figure 17a and c). Consistent with the transient transfection studies, galectin-3 expression was significantly lower ($p < 0.05$, $n = 3$; Figure 17b and c), approaching levels observed in MCF-12A HMECs, in MDA-MB-231 cells stably expressing U6-shRNA-Chk compared to empty-vector control cells (Figure 17b and c).

This change in the differentiation marker galectin-3 is consistent with a significant increase of lipid droplets detected by Nile red staining and an increase of the lipid triacylglyceride signal in lipid extract ^{1}H MR spectra.[66] Because the mammary gland utilizes lipid droplets for the production of milk,[74] these triacylglycerol-containing lipid droplets are a marker of human breast epithelial cell differentiation.[75,76] Other possible explanations are that excess 1,2-diacylglycerol, formed following choline kinase downregulation, may be stored in the form of lipid droplets, potentially detoxifying cells from excess 1,2-diacylglycerol,[77,78] or that the observed lipid droplet formation was a stress response.[79−81]

Conclusions

The data presented here demonstrate the strong association between malignant changes and choline phospholipid metabolism. Knocking down choline kinase induced a profound change in proliferation and differentation of invasive and metastatic breast cancer cells. Choline kinase is by no means the only target that can be utilized against cancer cells. Microarray analyses of a panel of malignant and nonmalignant HMECs have revealed at least two or more overexpressed enzymes as well as three or more underexpressed enzymes (see Table 3) that, targeted in vivo by siRNA or cDNA either singly or multiply using viral or liposomal delivery mechanisms, may prove effective for cancer-specific therapy. In addition, genomic characterization of the molecular basis of the reduction in total choline in responding tumors will provide further insight into new molecular targets for cancer therapy.

Acknowledgment. The work described in this contextual review was supported by P50 CA103175, R01 CA73850, and R01 CA82337.

MP060067E

(70) Honjo, Y.; Nangia-Makker, P.; Inohara, H.; Raz, A. *Clin. Cancer Res.* **2001**, *7*, 661−8.
(71) Takenaka, Y.; Fukumori, T.; Raz, A. *Glycoconj. J.* **2004**, *19*, 543−9.
(72) Iurisci, I.; Tinari, N.; Natoli, C.; Angelucci, D.; Cianchetti, E.; Iacobelli, S. *Clin. Cancer Res.* **2000**, *6*, 1389−93.
(73) Perillo, N. L.; Marcus, M. E.; Baum, L. G. *J. Mol. Med.* **1998**, *76*, 402−12.
(74) Mather, I. H.; Keenan, T. W. *J. Mammary Gland Biol. Neoplasia* **1998**, *3*, 259−73.
(75) Guilbaud, N. F.; Gas, N.; Dupont, M. A.; Valette, A. *J. Cell Physiol.* **1990**, *145*, 162−72.
(76) Munster, P. N.; Srethapakdi, M.; Moasser, M. M.; Rosen, N. *Cancer Res.* **2001**, *61*, 2945−52.
(77) Bell, R. M.; Coleman, R. A. *Annu. Rev. Biochem.* **1980**, *49*, 459−87.
(78) Lehner, R.; Kuksis, A. *Prog. Lipid Res.* **1996**, *35*, 169−201.
(79) Delikatny, E. J.; Roman, S. K.; Hancock, R.; Jeitner, T. M.; Lander, C. M.; Rideout, D. C.; Mountford, C. E. *Int. J. Cancer* **1996**, *67*, 72−9.
(80) Sathasivam, N.; Brammah, S.; Wright, L. C.; Delikatny, E. J. *Biochim. Biophys. Acta* **2003**, *1633*, 149−60.
(81) Delikatny, E. J.; Cooper, W. A.; Brammah, S.; Sathasivam, N.; Rideout, D. C. *Cancer Res.* **2002**, *62*, 1394−400.